J Fluoresc (2011) 21:1337–1342
DOI 10.1007/s10895-011-0864-9

SHORT COMMUNICATION

Intense Upconversion Luminescence of Yb^{3+}-Er^{3+} in Li_2O Content Tungsten-tellurite Glasses

Ghizal F. Ansari · Sachin Kumar Mahajan · J. Parashar

Received: 26 November 2010 / Accepted: 13 February 2011 / Published online: 2 March 2011

Abstract The Er^{3+} -Yb^{3+} codoped in Li_2O content tungsten -tellurite (TWL) transparent glasses are synthesized and measured the absorption, Raman and upconversion luminescence (UPL) spectra. At room temperature intense green emission peak at 560 nm ($^4S_{3/2}\rightarrow{}^4I_{15/2}$) and red emission peak at 670 nm ($^4F_{9/2}\rightarrow{}^4I_{15/2}$) of Er^{3+} observed even at minimum 86 mW pumping power of infrared 980 nm excitation. For structure of the TWL glass, Raman spectrum result revealed that an important role of WO_3 in the formation of glass network linkage with Li_2O. Under this influence estimated lifetime of the $^4I_{11/2}$ of Er^{3+} was 1.89 μs and due to lower phonon energy of the glass produce strong upconversion signal. The effect of Er_2O_3 concentration on emission intensity result indicated that green emission intensity initially increase in compare to red emission. Under the 980 nm pump power variation measured the relatively increases the red emission to the green emission intensity and analyze the possible upconversion mechanism and process.

Keywords Lanthanide ion-doped tellurite glasses · Optical properties erbium · Upconversion luminescence · Raman spectrum

Introduction

The trivalent rare-earth ions such as Er^{3+}, Tm^{3+},Ho^{3+}, $Pr^{3+}$and Nd^{3+} doped materials have scientific and technological interest due to their optical properties in developing photonic devices, compact laser and broad band amplifier [1–3]. Among the rare-earth ions, Er^{3+} is most popular as well as most efficient ions. In addition with Yb^{3+} ions as a sensitizer, perform an important role to improve the energy transfer to Er^{3+} ions and luminescence efficiency accordingly [4, 5]. The host material for rare-earth ions play an important role in obtaining efficient upconversion signal, since glass host with low phonon energy can reduce nonradiative loss to multiphonon relaxation and thus realize strong upconversion luminescence [6–8]. Generally, upconversion is difficult to observe in observe in oxide crystals or glasses compared with that fluoride glasses. But oxide glasses might be much better for practical applications because of their high thermal stability, chemical durability and ease of fabrication [9, 10].

In recent years, tellurite glasses are growing interest due to their low phonon energy of 600–800 cm^{-1}, which is significantly lower than that of both silicates (1,100 cm^{-1}) and germinates (880 cm^{-1}), and the large refractive index (>2.0) enhances both the absorption and emission cross sections [11, 12]. Also tellurite glasses are more chemically and environmentally stable than fluoride glasses, and have high rare-earth ions solubility. This has promoted a widespread interest in the spectroscopy investigation of tellurite glasses, especially the composition based on tungsten tellurite [13]. Comparing with sodium-tellurite and zinc-tellurite glasses have relatively low T_g and but better thermal stability which will helpful for fiber drawing [14]. Further crystals or glasses with addition of certain alkalie oxide as the network modifier could enhance the optical properties. Chen et al. observed enhanced upconversion emission in Y_2O_3 nanocrystal by codoping with Li^{3+} ions [15]. Shen et al. reported that Er^{3+} in tungsten-tellurite glasses mainly in the TeO_2-WO_3-R_2O(R=K, Na,

G. F. Ansari · S. K. Mahajan (✉) · J. Parashar
Department of Applied Physics,
Samrat Ashok Technological Institute,
Vidisha, MP 464001, India
e-mail: sachin_k_mahajan@rediffmail.com

Li) glasses for 1.5 μm emission for optical amplifier [16]. No publications concerned with upconversion fluorescence of Er^{3+}/Yb^{3+} in Li_2O-WO_3-TeO_2 glasses have come to our notice, though structural study in different composition for same content of this glasses by X-ray photoelectron spectroscopy and Raman spectra have been reported [17, 18].

This work deals with the synthesis, structural and optical measurements of glass samples of Er^{3+}/Yb^{3+} codoped $68TeO_2$-$15Li_2CO_3$-$13WO_3$ (TWL) system. The 15 mol% content of Li_2O was chosen because Na_2O-TeO_2 glasses show marked stability which is compositional-dependent with maximum at 20 mol% fraction of Na_2O [19]. Green and red emission of glass samples under the 980 nm excitation was measured to verify visible upconversion via energy transfer process from Yb^{3+} to Er^{3+} and possible upconversion mechanisms are discussed.

Experimental

The basic composition of the glass sample was $(70\text{-}x)TeO_2$-$15Li_2CO_3$-13 WO_3- $2Yb_2O_3$ (in mol%) where x range mixed with Er_2O_3 (Fluka 99.99%) concentration from 0.5 to 2 mol%. For undoped lithium tungsten tellurite glass sample composition was $70TeO_2$-$15Li_2CO_3$-$15WO_3$ prepared for the Raman spectrum. All the starting constituents materials were purer than 99.9 %(TeO_2 Aldrich, Li_2CO_3 Otto, WO_3 Otto and Yb_2O_3 Fluka) in batch of 10gm was mixed in agate mortar and melted in alumina crucible with lid at temperature range 850–950 °C about 30–45 min in muffle furnaces at air atmosphere. The homogeneous and transparent form of glass disc of 6 mm in diameter and 1–1.5 mm thickness were obtained by pouring quickly the glass liquid into preheated stainless steel sheet plates. As made glasses were annealed below the glass transition temperature at 310 °C for 8 h and allowed to cool at room temperature to obtain transparent light pink colour samples for subsequent measurements.

The density of TWL: Er/Yb glass sample was measured according to the Archimedes's principle using water as an immersion liquid, to be 4.87gm cm^{-3}. The refractive index was measured by Brewster angles method using a spectrometer with sodium –vapor lamp is 2.1. The Raman spectrum of the undoped TWL glass sample was measured by Raman spectrophotometer (Andor Technology SR370I) with diode laser at 758 nm was used as an incident light source. The visible and near –infrared absorption spectra of the glass sample was measured at room temperature using atomic absorption spectrophotometer(GBC Australia) over spectral range of 300–850 nm. The upconversion emission spectra were obtained with SEPEX Fluorolog 1680 (0.22 m double beam) spectrometer upon 980nm diode laser (Scitec Instrument, UK) excitation adjustable to maximum power of 1 W. In order to compare the upconversion luminescence intensity of different Er_2O_3 with fixed Yb_2O_3 doped TWL glass samples as accurate as we can the position, power (200 mW) of pumping beam and width of slit to collect the luminescence signal were fixed to same condition and the sample was set at the same place in the experimental setup.

Results and Discussions

Absorption Spectrum

Figure 1 shows the absorption spectra for TWL: Er/Yb glass sample at room temperature. The absorption spectra of Er^{3+} ion consists of eight absorption bands centered at 800 nm,650 nm, 540 nm, 520 nm, 490 nm,451 nm,406 nm, 377 nm corresponding to the absorption from the ground state $^4I_{15/2}$ to the excited states $^4I_{9/2}$,$^4F_{9/2}$,$^4S_{3/2}$,$^2H_{11/2}$,$^4F_{5/2}$+$^4F_{3/2}$, $^2H_{9/2}$,$^4G_{11/2}$ respectively. The absorption bands below 377 nm cannot be observed because of the band gap of the glass matrix and spectroscopic measurement was limited due to upper limit of spectrophotometer at 850 nm. However intense absorption band at the wavelength region from 950 nm to 1050 nm may be observed due to the large contribution of the absorption of $Yb^{3+}$and Er^{3+}, which arise from the transition $^2F_{7/2}\rightarrow{}^2F_{5/2}$ and $^4I_{11/2}\rightarrow{}^4I_{15/2}$ respectively as the band positions for Er^{3+}-Yb^{3+} are similar to halide modified tellurite glasses [20]. Thus the samples present a good transparency in visible region indicating that possibility of practical applications in the visible region and negligibility of energy transfer from Er^{3+} to the glass matrix.

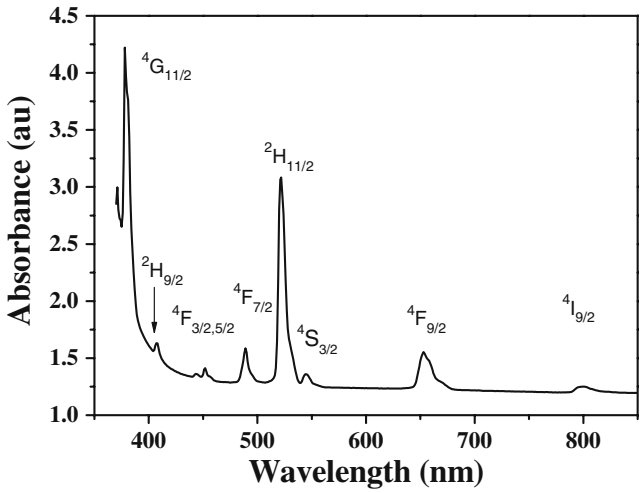

Fig. 1 Absorption spectrum of $68TeO_2$-$15Li_2CO_3$-$13WO_3$: 2Er-2Yb (mol%) glass

Raman Spectrum of Undoped TWL Glass

Figure 2 shows the room temperature fluorescence subtracted Raman spectrum of undoped TWL glass. The Raman spectrum indicates the phonon frequency band peaked at 760 cm^{-1} and 930 cm^{-1} correspond to TeO_2 and WO_3 vibration respectively. The 760 cm^{-1} attributed to that of TeO_3 trigonal pyramid (tp) units due to stretching vibrations of TeO_3 and /or TeO_{3+1}. The highest peak at about 930 cm^{-1} is observed corresponds to the stretching vibrations of W=O and W-O^- bonds associated with WO_4 and WO_6 groups. This mean that addition of WO_3 into TeO_2 result in the reduction of Te-O-Te linkages, and the formation of W-O-W and W-O-Te linkages [21]. These bands are similar and nearly same position of peaks was reported in the Raman spectrum of $85.5TeO_2$-$12.5WO_3$ glass [22, 23]. But in our measurement side band near about 600 cm^{-1} could not be observed due to lower limit of used Raman Spectrometer measurements. However, the Raman vibration at 460 cm^{-1} is attributed to Te-O-Te chain unit symmetric stretching mode, while the spectral features from 610 cm^{-1} to 680 $cm^{-1}$and 760 cm^{-1} correspond to TeO_4 bi-pyramidal arrangement and TeO_3(and /or TeO_{3+1}) trigonal pyramids structure, respectively [24]. In our Li_2O modified in tungsten tellurite glasses, negligible shift of TeO_4 band is observed in Fig. 2. Moreover, the intensity of bands at 460 cm^{-1} decrease which indicates the Te-O-Te linkage becoming increasing more depolymerized as TeO_4 is converted to TeO_3 with addition of Li_2O. Also in addition of Li_2O to tungsten tellurite (in between 10 and 15 mol%) results in a decrease of glass transition temperature due to the cleavage of the networks formed by TeO_4 trigonal bipyramid units and the increase of nonbridging oxygen (NBO) atoms [25], and W-O stretching shift also change.

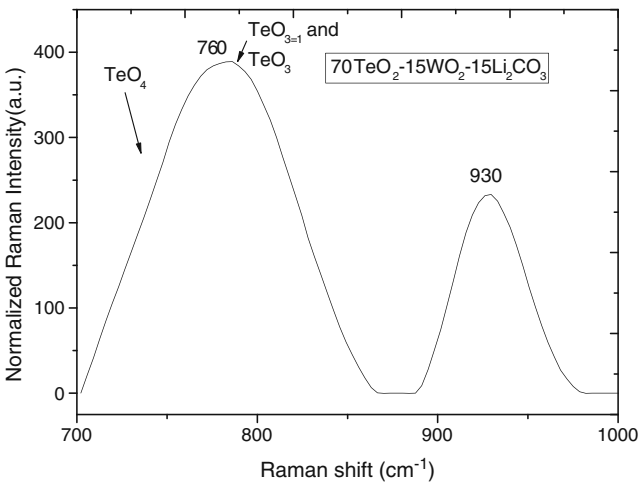

Fig. 2 Raman spectrum of the undoped TWL glass

In the TWL glass, Er^{3+} ions are surrounded by NBO of TeO_4 tetrahedra and energy of local vibrational mode coupled to the Er^{3+} centers could be smaller than that of the maximum phonon energy of glass network. As per observed result the phonon energy of tungsten –tellurite glass is evidently larger than that of tellurite glass at 750 cm^{-1}. In our case change in energy transfer in Er^{3+} caused by the substitution of alkali ions can be neglected because maximum phonon energy are kept unchanged. The lifetime of the $^4I_{11/2}$ level of Er^{3+} in TWL tellurite glasses may be determined almost entirely by the non-radiative decay rate [26]. Since energy gap of transition $^4I_{11/2} \rightarrow {}^4I_{15/2}$ is about 3,600 cm^{-1} then the non –radiative transition rate can be descried as

$$\tau^{-1} = W_{non-rad} \approx 10^7 \exp[-2(p - 2.4)], \quad (1)$$

where, $p=\Delta E/\hbar\omega$ is the number of phonon energy $\hbar\omega$ required to bridge the energy ΔE. Thus from the calculation of lifetime of the $^4I_{11/2}$ level of Er^{3+} in TWL glass is ~1.89 μs, and that of tellurite glass is 12 μs, and that of silica glass is close to 1 μs. In fact, the lifetime of $^4I_{11/2}$ level of Er^{3+} in TWL glass is comparable to that of silica glass, so it is possible to pump efficiently at 980 nm and excite ground level $^4I_{15/2}$ to upper level $^4I_{11/2}$ of Er^{3+}ions. Thus the enhanced green and the red radative transitions were observed from the reduced non-radiative transition in the TWL glass system. Further this TWL glsass for 1.5 μm emission may be used by introduction of high phonon energy oxide such as P_2O_5, which increased the non-radiative decay rate of Er^{3+} ions and reduced the upconversion luminescence.

Upconversion Fluorescence and Mechanism

Figure 3 presents the upconversion emission spectra of the TWL: Er^{3+}/Yb^{3+}(2 mol%:2 mol%) glass sample in the wavelength range of 500–700 nm under 980 nm diode laser excitation at room temperature. The observed upconversion luminescence of intense green and red spectral bands has peaks at wavelength 540 nm with small shoulder at 525 nm, and 670 nm with shoulder 640 nm are simultaneously observed. The wavelength 540 nm and 525 nm corresponds to Er^{3+}: $^4S_{3/2} \rightarrow {}^4I_{15/2}$, $^2H_{11/2} \rightarrow {}^4I_{15/2}$ transition respectively while both 670 nm and 640 nm corresponding to $^4F_{9/2} \rightarrow {}^4I_{15/2}$ transition. With increasing the excitation intensity on measurement of emission intensity upconversion red emission intensity relatively increases to the green emission. However green emission is bright enough to be perceived with the naked eye even at low pump power (86 mW). It is also noted that red and green emission bands present considerably large half widths (5 nm around 520 nm, 16 nm around 560 nm, and 23 nm around 670 nm) due to the high

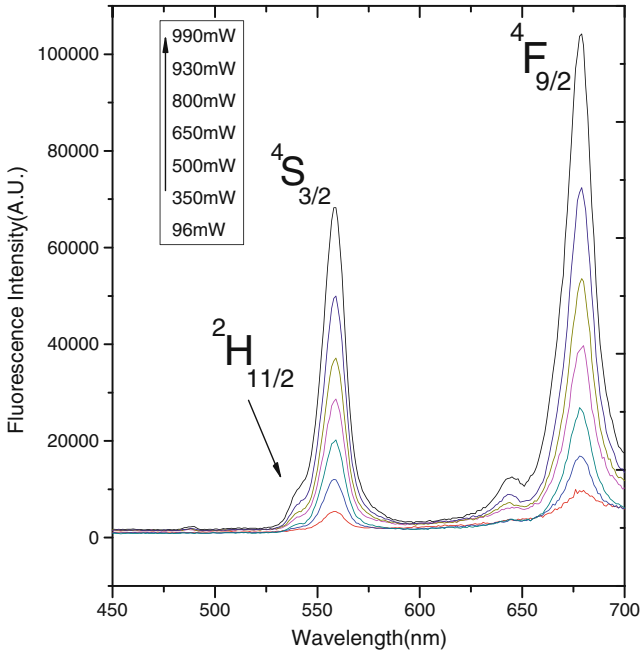

Fig. 3 Upconversion fluorescence spectra of TWL: Er (2 mol%)-Yb (2 mol%) glass at room temperature

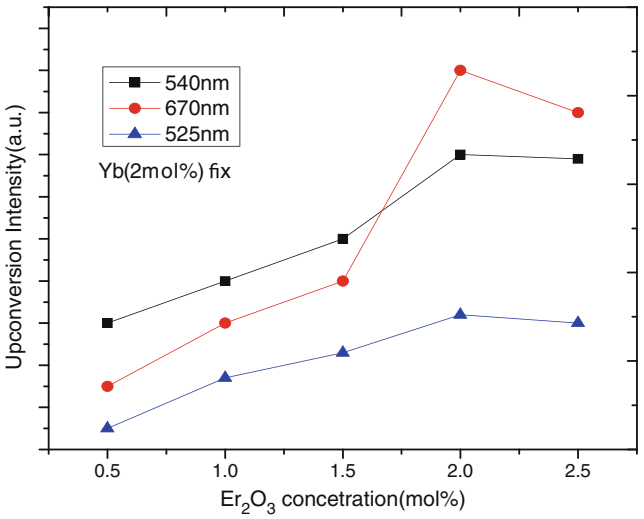

Fig. 4 Upconversion luminescence intensities as a function of Er_2O_3concentration at fix Yb_2O_3(2 mol%)

local heating of the sample, caused by efficient 980 nm absorption by Yb^{3+} ions. These visible emissions not only are lower Stark components of the emitting levels $^2H_{11/2}$, $^4S_{3/2}$ and $^4F_{9/2}$ responsible for emission, but also upper ones, which are thermally populated.

To obtain the optimum doping concentration of Er^{3+} ions, a series of glasses doped with different Er^{3+} concentration were prepared, in which the Yb_2O_3 content were all 2 mol% fraction. When increasing the Er^{3+} concentration, the fluorescence intensity increases at the beginning due to an increasing absorption of pump energy and energy transfer from Yb^{3+} to Er^{3+} as shown in Fig. 4. On comparison the emission intensity for concentration of Er_2O_3 at 200mw pump power, Initially green emission intensity increase unto 1 mol% and then gradually red emission at 670 nm increase unto 2 mol%. The plot clearly shows that the glass containing 2 mol% of Er^{3+} ions is best upconversion emission intensity of TWL glass. And when Er^{3+} concentration is beyond a 2 mol% concentration, the intensity remain constant and/or decreases. This stronger red emission observed due to shortened distance between Er^{3+} ions at higher concentration. We assume that too much Yb^{3+} ions will cause the increase in back energy transfer from Er^{3+} to Yb^{3+}, i.e. $.^4I_{11/2}(Er^{3+})+^2F_{7/2}(Yb^{3+}) \rightarrow ^4F_{15/2}(Er^{3+})+^2F_{5/2}(Yb^{3+})$. In addition, the up conversion intensities of Er^{3+} ions will become stronger with increasing Yb^{3+} ions in the TWL glass.

Figure 5 depicts the log-log dependence of the integrated green (540 nm) and red(670nm) emission intensities on the excitation power at 980 nm. The Upconversion intensity $\boldsymbol{I_{UP}}$ will be proportional to m^{th} power of the $\boldsymbol{I_{IR}}$ excitation Intensity i.e. $I_{UP} \propto I_{IR}^m$, where, m is the number of $\boldsymbol{I_{IR}}$ photons required to convert a visible photon. A plot of ln ($\boldsymbol{I_{UP}}$) versus ln ($\boldsymbol{I_{IR}}$) yields a straight line with slope m of which the value is obtained from the slope of the graph [27]. Such dependence of integrated green and red emission intensities $\boldsymbol{I_{UP}}$ on excitation power intensity $\boldsymbol{I_{RI}}$ present in Fig. 5, which indicate that for the green and red emission for Er^{3+}/Yb^{3+} (2 mol%:2 mol%) codoped lithium tungsten tellurite glass has given the straight lines with slop of 2 and 2.1 respectively. The results confirm that a two- photon upconversion process is assigned to the green and red

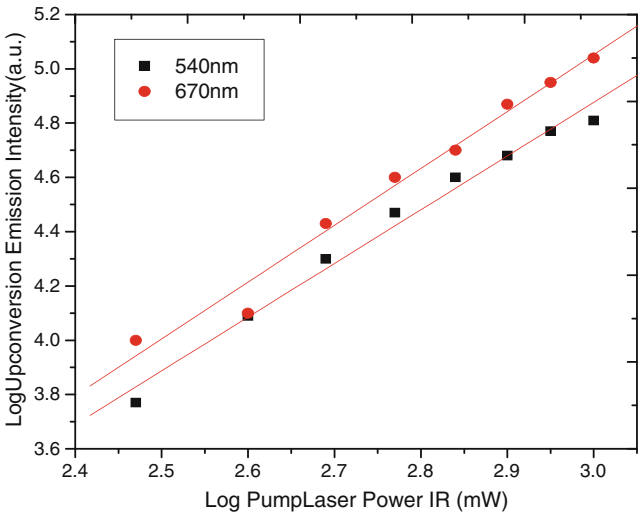

Fig. 5 Dependence of red and green upconversion fluorescence intensity on 980 nm LD excitation pump power for TWL glass

emission from, $^4S_{3/2}$ and $^4F_{9/2}$ level of Er^{3+} respectively. Based on the energy matching conditions and the dependence on excitation power, the possible upconversion mechanisms for the emission bands are discussed based on the energy level of Er^{3+} and Yb^{3+} ions presented in Fig. 6. Usually, the up-conversion emission of Er^{3+} can be explained by several well- known mechanisms such as excited –state absorption (ESA), energy transfer up-conversion (ETU) [27]. In singly Er^{3+} ions doped glass samples with 980 nm photons are responsible for excitation of the $^4I_{11/2}$ level which can also populate the lower-lying $^4I_{13/2}$ through multiphonon decay. Besides possibly originating near-infrared emission around 1550 nm and 2800 nm, both these metastable levels can undergo ESA of 980 nm photons leading to excitation of upper $^4F_{9/2}$ and $^4F_{7/2}$ levels. Given the small energy gap separating the levels $^4F_{7/2}$ and ($^2H_{11/2}$, $^4S_{3/2}$), the latter are rapidly populated via multiphonon decay from $^4F_{7/2}$. In ETU process involves not only two closely neighboring Er^{3+} ions but also in Er^{3+} and Yb^{3+} ions. In Er^{3+}/Yb^{3+} co-doped samples the Yb→Er energy transfers (ET_1, ET_2 and ET_3 in Fig. 6) are known to be the most significant contribution for 980 nm upconversion excitation. For the green emissions, in first step, the $^4I_{11/2}$ level is directly excited with 980 nm light ground state absorption process (GSA) and /or by energy transfer (ET) process from $^2F_{5/2}$ level of Yb^{3+}: $^2F_{5/2}(Yb^{3+})$+ $^4I_{15/2}(Er^{3+})$→ $^2F_{7/2}(Yb^{3+})$+$^4I_{11/2}(Er^{3+})$. Since Yb^{3+} has a much large absorption cross-section than Er^{3+} in the 980 nm region, the ET process is dominated to the excitation of $^4I_{11/2}$ level. Thus the second step involved the excitation process based on long–lived $^4I_{11/2}$ level as follows: cross-relaxation(CR), $^4I_{11/2}(Er^{3+})$+$^4I_{11/2}(Er^{3+})$ → $^4F_{7/2}(Er^{3+})$+$^4I_{15/2}(Er^{3+})$; excited state absorption (ESA),$^4I_{11/2}(Er^{3+})$+ a photon→$^4F_{7/2}(Er^{3+})$; ET, $^2F_{5/2}(Yb^{3+})$+$^4I_{11/2}(Er^{3+})$ →$^2F_{7/2}(Yb^{3+})$+$^4F_{7/2}(Er^{3+})$. The populated $^4F_{7/2}$ level of Er^{3+} then relaxes rapidly and nonradiatively to the next lower level $^2H_{11/2}$ and $^4S_{3/2}$ resulting form the small energy gap between them. The $^2H_{11/2}$ state can also decay to the $^4S_{3/2}$ state due to multiphonon relaxation process. It is found that estimated energy gap between the $^2H_{11/2}$ and next lower level state $^4S_{3/2}$ is ~800 cm^{-1} [28], thus the multiphonon relaxation rate is very large and $^2H_{11/2}$→$^4I_{15/2}$ transition is reduced. The above process produced the $^4S_{3/2}$→$^4I_{15/2}$ transition for green emission centered at 540 nm. In our experiment with increasing Er_2O_3 concentration, the energy transfer rate increases, via Yb^{3+} and thus the visible emissions intensity increases. Therefore, the nonradiative transition rate through multiphonon relaxation from $^4S_{3/2}$ becomes smaller than from $^2H_{11/2}$, and the upconversion intensity from $^4S_{3/2}$→$^4I_{15/2}$ transition is larger than from $^2H_{11/2}$ →$^4I_{15/2}$ transition as this result obtained for composition of $68TeO_2$-$15Li_2CO_3$-$13WO_3$: $2Yb_2O_3$-$2Er_2O_3$ glass.

The red upconversion emission is originated form the $^4F_{9/2}$→$^4I_{15/2}$ transition centered at 670 nm and there exist two possible pumping mechanisms. The first pumping mechanism comprises the population of the $^4S_{3/2}$ state, followed by a fast nonradiative decay through multiphonon interaction from the population $^4S_{3/2}$ level to $^4F_{9/2}$ level and

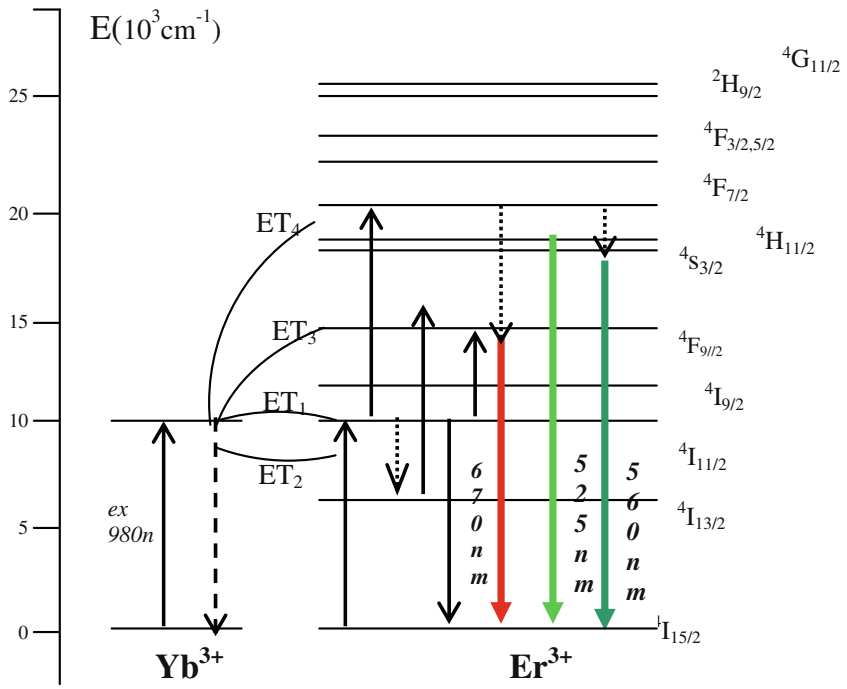

Fig. 6 Partial energy level diagrams of Er^{3+} and Yb^{3+}. The pumping transition at 980 nm along with the up conversion emission in the green and red spectral region

then to the ground state. In other possible mechanism the population of $^4F_{9/2}$ is based on the processes as follows: ET from Yb^{3+}, $^2F_{5/2}(Yb^{3+})+^4I_{13/2}(Er^{3+}) \rightarrow {}^2F_{7/2}(Yb^{3+}) + {}^4F_{9/2}(Er^{3+})$; cross relaxation between Er^{3+} ions, $^4I_{13/2}+{}^4I_{11/2}\rightarrow {}^4I_{15/2}+{}^4F_{9/2}$; ESA, $^4I_{13/2}+$ a Photon$\rightarrow {}^4F_{9/2}$. The $^4I_{13/2}$ level is populated owing to the nonradiative relaxation from the upper $^4I_{11/2}$ level. Additional non-radiative decay form $^4S_{3/2}$ can also populate level $^4F_{9/2}$ favoring the red emission ($^4F_{9/2}\rightarrow {}^4I_{15/2}$). At Er_2O_3 concentration is high enough that allow the interaction of these ions and various cross- relaxation energy transfers involving levels $^4I_{11/2}$ and $^4I_{13/2}$, playing a role in the excitation to the upper levels. Further relative increase of the red emission intensity to the green emission at higher 2 mol% Er^{3+} indicated the short distance between Er^{3+} ions benefit the red emission [29, 30]. In our TWL glass composition with higher concentration of Li_2O (15 mol%) may promote the formation of new impurity phase which might benefit the aggregation of Er^{3+} ions and the rate of cross relaxation energy transfer between Er^{3+}ions would be improved resulting in the red emission being enhanced again. Thus the TWL is more preferable for red emission than green emission on pump power variation. However almost another oxide based Er^{3+}/Yb^{3+} codoped tellurite glass matrix dominated green emission intensity upon 980 nm excitation [12]. This characteristics of Li_2O modified in tungsten tellurite glass has never been reported in other $Er^{3+/}Yb^{3+}$ codoped tellurite based glass materials pumped at around 980 nm.

Conclusions

Er^{3+}/Yb^{3+} co-doped modified tungsten tellurite by Li_2O glasses have been fabricated and characterized for absorption, Raman and upconvesion luminescence spectrum. The analysis of Raman spectrum confirms Li_2O enters as an intermediate between a network formerTeO_2 and a network modifier WO_3, as a result W-O stretching-band shift has been observed in undoped TWL. The maximum phonon energy of TWL glass measured about 930 cm^{-1}, which leads to estimated lifetime of $^4I_{11/2}$ of Er^{3+}ions~1.89 μs. With increasing Er_2O_3 at fix Yb_2O_3(2 mol%) in TWL glass matrix, the intensity green emission at 525 nm increase slightly and560nm increases largely while red emission at 670 nm increase more than that of green at 2 mol% of Er_2O_3. Under 980 nm pump power variation for TWL :2Er-2Yb(mol%) glass sample shows relatively increase of intense red at 670 nm to green at 560 nm emissions indicate the quadratic dependent of upconversion intensity on pump intensity. The enhancement of red emission with increasing Er^{3+} ion concentration is due to cross-relaxation process. Thus it is found that TWL glass system may is considered for upconversion device although it is most prospective material for fiber and amplifier. The Judd-Ofelt intensity parameter and radiative lifetime estimation will be in progress in next work.

Acknowledgments This work was financially supported by AICTE (RPS) New Delhi, grant (No. 8023/BOR/RPS-198).The authors would like thank P.K.Gupta & H.S.Patel RRCAT(Govt. of India) Indore, India for cherterization and spectral measurements.

References

1. Chrysswou CE, Kenyon AJ, Smeeton TM, Humphreys CJ, Hole DE (2004) App Phys Lett 85:5200
2. Peng X, Song F, Kuwata-Gonokami M, Tiang S, Peyghambarian N (2003) App Phys Lett 83:5380
3. Biswas A, Maciel GS, Kapoor R, Friend CS, Prasad PN (2003) Appl Phys Lett 82:2389
4. Strohhoter C, Polman A (2001) J App Phys 90:4314
5. Laporta P, de Silvestri S, Magni V, Svelto O (1991) Opt Lett 16:1952
6. Gapobianco A, Prevost G, Proutx PP, Bettinelli M (1996) Opt Mat 6:175
7. de Araujo CB, Menezes LS, Maciel GS, Acioli LH, Gomes ASL, Messaddeg Y, Florez A, Aeqerter A (1996) App Phys Lett 68:602
8. Hehlen MP, Cockroft NJ, Gosnell TR, Bruce AJ, Nykolak G, Jshmulovich (1997) Opt Lett 22:772
9. Feng X, Tanabe S, Hanada T (2001) J Appl Phys 89:3560
10. Wang GN, Xu SQ, Yang JH et al (2004) J Non-Cryst Solids 336:102
11. Nunzi Conti G, Berneschi S, Bettinelli M, Brenci M, Chen B, Pelli S, Speghini A, Righini GC (2004) J Non-Cryst Solid 345–346:343
12. Park KK, Choi HY, Kim JH (2004) Sae Mulli (South Korea) 48:560
13. Lakshminarayana G, Jianrong Qiu, Brik MG, Kumar GA, Kityk IV (2008) J Phys Condens Matter 20:375110
14. Feng X, Qi C, Lin F, Hu H (1999) J Non-Crystal Solid 256&257:372–377
15. Zhang ZG, Sun Q, Wang FP (2008) Applied Physics Lett 92:113114
16. Shen S, Naftaly M, Jha A (2002) Opt Commun 205:101
17. Lim JW, Jain H, Toulouse J, Marjanovic S, Sanghera JS, Miklos R, Aggarwal ID (2004) J Non-Cryst Solids 349:60–65
18. Hager IZ, Mallawany REI (2010) J Mater Sci 45:897–905
19. Mclaughlin JC, Tagg SL, Zwanziger JW (2001) J Phys Chem B 105:67–75
20. Yang J, Zhang L, Wen L, Dai S, Hu L, Jiang Z (2004) J Appl Phys 95:3020
21. Zhao S, Wang X, Fang D, Xu S, Hu L (2006) J Alloys Compd 424:243
22. Plotnichenko VG, Sokolov VO, Koltashev VV, Dianov EM, Grishin IA, Churbanov MF (2005) Opt Lett 30:1156
23. Lin H, Wang X, Lin L, Li C, Yang D, Tanabe S (2007) J Phys D Appl Phys 40:3567
24. Murugan GS, Ohishi Y (2004) J Non-Cryst Solids 341:86
25. Sekiya T, Mochida N, Ohtsuka A, Tonokawa M (1989) J Ceram Soc Jpn 97:1435–1440
26. Imbush GF (1991) In: Di Bartolo B (ed) Advances in nonradiative processes in solids. Plenum Press, New York, p261
27. Sun HT, Dai SX, Xu SQ, Wen L, Hu LL, Jiang ZH (2004) Mater Lett 58:3948
28. Man SQ, Pun EYB, Chung PS (2000) Appl Phys Lett 77:483
29. Balda R, Fernandez J, Adam JL, Lacha LM, Arriandiaga MA (2003) J Non-Cryst Solids 326–327:330
30. Kanoun A, Jaba N, Brenier A (2003) Opt Mater Sci Eng B 97:11